



SOLID SOLUBILITY AND IONIC CONDUCTIVITY OF Li_3TaO_4 AND RELATED PHASES

SYAFIQAH BINTI SHARI

FS 2019 76



**SOLID SOLUBILITY AND IONIC CONDUCTIVITY OF Li_3TaO_4 AND
RELATED PHASES**

By

SYAFIQAH BINTI SHARI

**Thesis Submitted to the School of Graduate Studies, Universiti Putra
Malaysia, in Fulfilment of the Requirements for the Degree of Master of
Science**

November 2018

All material contained within the thesis, including without limitation text, logos, icons, photographs and all other artwork, is copyright material of Universiti Putra Malaysia unless otherwise stated. Use may be made of any material contained within the thesis for non-commercial purposes from the copyright holder. Commercial use of material may only be made with the express, prior, written permission of Universiti Putra Malaysia.

Copyright © Universiti Putra Malaysia



Abstract of thesis presented to the Senate of Universiti Putra Malaysia in Fulfilment of the requirement for the degree of Master of Science

SOLID SOLUBILITY AND IONIC CONDUCTIVITY OF Li_3TaO_4 AND RELATED PHASES

By

SYAFIQAH BINTI SHARI

November 2018

Chair : Tan Kar Ban, PhD
Faculty : Science

Lithium tantalate solid solution, $\text{Li}_{3+5x}\text{Ta}_{1-x}\text{O}_4$ was prepared by conventional solid-state reaction at 925°C over 48 h. The x-ray diffraction (XRD) analysis confirmed that these materials crystallised in a monoclinic symmetry, space group of $C2/c$ and $Z=8$, which was similar to the reported International Crystal Diffraction Database (ICDD), 98-006-7675. $\beta\text{-Li}_3\text{TaO}_4$ has a rock-salt structure with a cationic order of $\text{Li}^+ : \text{Ta}^{5+} = 3 : 1$ over the octahedral sites. The lithium solubility was investigated by varying the lithium content through a proposed formula, $\text{Li}_{3+5x}\text{Ta}_{1-x}\text{O}_4$ ($0 \leq x \leq 0.059$). Ac impedance study revealed that Li_3TaO_4 exhibited the highest conductivity, $3.82 \times 10^{-4} \text{ S cm}^{-1}$ at 600°C . The activation energy in the range $0.63 - 0.68 \text{ eV}$ were found in these materials.

In attempt to investigate the correlation between structural and electrical properties of the $\text{Li}_2\text{O-Ta}_2\text{O}_5$ systems, various chemical doping was performed. Tetravalent dopant, e.g. Ti^{4+} was introduced into the host structure with a proposed formula, $\text{Li}_3\text{Ti}_x\text{Ta}_{1-x}\text{O}_{4-x}$ ($0.45 \leq x \leq 0.75$) at same synthesis condition. The formation mechanism involved a one-to-one replacement to Ta^{5+} cation by Ti^{4+} cation with the creation of oxygen vacancy for charge compensation. The phase changed from an ordered monoclinic to a disordered cubic phase when x increased from 0 to 0.40. While, a disordered cubic Li_3TaO_4 phase was observed at $x = 0.45-0.75$. These materials were refined and fully indexed with a space group of $\text{Fm-}3\text{m}$, $Z=1$ with a slightly smaller lattice parameters, $a=b=c$, in the range $4.1907(2) - 4.1681(2) \text{ \AA}$. The unit cell contraction may be attributed to the replacement of larger Ta^{5+} (0.64 \AA) by a smaller Ti^{4+} (0.61 \AA) at the six-coordination. $\text{Li}_3\text{Ta}_{0.25}\text{Ti}_{0.75}\text{O}_{3.625}$ exhibited the highest conductivity among the Ti dopants at all temperatures, i.e. $2.33 \times 10^{-4} \text{ S cm}^{-1}$ at 600°C . The activation energies of these materials were estimated to be $1.16 - 1.32 \text{ eV}$.

On the other hand, an attempt was made to replace Nb by Ta using a proposed formula of $\text{Li}_3\text{Ta}_{0.5-x}\text{Nb}_x\text{Ti}_{0.5}\text{O}_{3.775}$. A complete substitutional solid solution was formed, which was mainly due to the similar chemical characteristics between these pentavalent cations. The lattice parameters $a=b=c$ were determined to be $4.1866(1) - 4.1849(4) \text{ \AA}$.

$\text{Li}_3\text{Ta}_{0.4}\text{Nb}_{0.1}\text{Ti}_{0.5}\text{O}_{3.75}$ ($x = 0.1$) was found to exhibit the highest conductivity, i.e. $1.78 \times 10^{-3} \text{ S cm}^{-1}$ at $600 \text{ }^\circ\text{C}$. The activation energies of these materials were estimated to be 1.35 - 1.49 eV.

Selected divalent cation dopants were chemically doped into the $\beta\text{-Li}_3\text{TaO}_4$ monoclinic phase. Both Mg and Zn dopants formed solid solutions with limit up to $x = 0.1$ only. The chemical formulae of $\text{Li}_{3-2x}\text{M}_x\text{TaO}_4$ ($\text{M} = \text{Mg}$ or Zn) was proposed wherein two Li^+ ions were substituted by a divalent M^{2+} cation. Both doped samples exhibited relatively higher conductivity than that of parent material, $\beta\text{-Li}_3\text{TaO}_4$. This was probably attributed to the creation of lithium vacancy or well-connected grain. The conductivity values of $\text{Li}_{2.8}\text{Mg}_{0.1}\text{TaO}_4$ and $\text{Li}_{2.8}\text{Zn}_{0.1}\text{TaO}_4$ were determined to be $3.60 \times 10^{-4} \text{ S cm}^{-1}$ and $5.99 \times 10^{-4} \text{ S cm}^{-1}$ at $600 \text{ }^\circ\text{C}$, respectively. Their resulted activation energies did not change significantly but remained reasonably low, i.e. 0.55 - 0.58 eV.

All the prepared samples appeared to be thermally stable as there are not thermal event detect in both TGA and DTA thermograms. The chemical stoichiometry of these samples was confirmed by ICP-OES, in which comparable values between theoretical and experimental concentrations were obtained. Structural analysis by FT-IR disclosed that several metal-oxygen bonds were found in the wavenumber range $250 - 1000 \text{ cm}^{-1}$. The irregular shaped grains in the range $0.95 - 10.82 \text{ }\mu\text{m}$ were also shown by the SEM micrographs. This was further supported by TEM analysis as the results showed some spherical particles with quadrangle edges were found in the samples.

In attempts to investigate the possibility of new solid solution formation and to determine the electrical performance of the $\text{Li}_2\text{O-Ta}_2\text{O}_5$ materials, chemical dopants were performed. These materials showed different solid solution limit and moderate lithium ionic conductivity

Abstrak tesis yang dikemukakan kepada Senat Universiti Putra Malaysia sebagai memenuhi keperluan untuk Ijazah Master Sains

KELARUTAN PEPEJAL DAN KEKONDUKSIAN ION BAGI Li_3TaO_4 DAN FASA-FASA BERKAITAN

Oleh

SYAFIQAH BINTI SHARI

November 2018

Pengerusi : Tan Kar Ban, PhD
Fakulti : Sains

Larutan pepejal litium tantalat, $\text{Li}_{3+5x}\text{Ta}_{1-x}\text{O}_4$ telah disintesis secara tindak balas keadaan pepejal pada suhu $925\text{ }^\circ\text{C}$ dalam 48 jam. Analisis belauan sinar-x (XRD) telah mengesahkan bahan-bahan mengahablur dalam simetri monoklinik, kumpulan ruang $C2/c$ dan $Z=8$ seperti yang telah dilaporkan di dalam Pangkalan Data Belauan Kristal Antarabangsa (ICDD), 98-006-7675. $\beta\text{-Li}_3\text{TaO}_4$ mempunyai struktur garam batuan dengan tertib kation Li^+ dan Ta^{5+} 3:1 pada tapak oktahedron. Keterlarutan litium telah dikaji dengan pengubahan kandungan litium secara formula, $\text{Li}_{3+5x}\text{Ta}_{1-x}\text{O}_4$ ($0 \leq x \leq 0.059$). Kajian ac impedans Li_3TaO_4 menunjukkan kekonduksian yang paling tinggi, $3.82 \times 10^{-4} \text{ S cm}^{-1}$ pada $600\text{ }^\circ\text{C}$. Tenaga pengaktifan dalam julat $0.63 - 0.68 \text{ eV}$ ditentukan untuk bahan-bahan ini.

Dalam usaha untuk mengkaji korelasi diantara sifat struktur dan elektrik sistem $\text{Li}_2\text{O-Ta}_2\text{O}_5$, pelbagai pendopan kimia telah dibuat. Dopan tetravalensi, Ti telah diperkenalkan ke dalam struktur perumah dengan mekanisme, $\text{Li}_3\text{Ti}_x\text{Ta}_{1-x}\text{O}_{4-x}$ ($0.45 \leq x \leq 0.75$) pada keadaan sintesis yang sama. Mekanisme pembentukan melibatkan penggantian satu kation Ta^{5+} dengan satu kation Ti^{4+} dan juga kekosongan oksigen demi pampasan cas. Peralihan fasa dari monoklinik teratur kepada kubik yang tak teratur berlaku apabila x meningkat dari 0 hingga 0.40. Manakala, fasa kubik Li_3TaO_4 tak teratur ditemui pada $x = 0.45-0.75$. Bahan-bahan ini telah diindeks sepenuhnya dengan kumpulan ruang, $\text{Fm-}3m$, $Z=1$ dan juga pengecilan parameter kekisi, $a=b=c$, yang berada dalam julat $4.1907(2) - 4.1681(2) \text{ \AA}$. Penyusutan sel unit adalah disebabkan oleh penggantian saiz jejari ion Ta^{5+} (0.64 \AA) yang lebih besar jika dibandingkan dengan Ti^{4+} (0.61 \AA) pada koordinasi-enam. $\text{Li}_3\text{Ta}_{0.25}\text{Ti}_{0.75}\text{O}_{3.625}$ menunjukkan nilai kekonduksian yang paling tinggi di antara dopan Ti pada semua suhu, iaitu $2.33 \times 10^{-4} \text{ S cm}^{-1}$ pada $600\text{ }^\circ\text{C}$. Tenaga pengaktifan untuk bahan-bahan telah dianggarkan dalam julat $1.16 - 1.32 \text{ eV}$.

Selain itu, satu percubaan telah dilakukan untuk menggantikan Nb dengan Ta secara formula, $\text{Li}_3\text{Ta}_{0.5-x}\text{Nb}_x\text{Ti}_{0.5}\text{O}_{3.775}$. Larutan pepejal penggantian yang lengkap telah

dihasilkan atas sebab ciri kimia yang sama di antara kation pentavalensi. Parameter kekisi, $a=b=c$, telah ditentukan dalam julat 4.1866(1) - 4.1849(4) Å. $\text{Li}_3\text{Ta}_{0.4}\text{Nb}_{0.1}\text{Ti}_{0.5}\text{O}_{3.75}$ ($x = 0.1$) menunjukkan nilai kekonduksian yang paling tinggi di antara dopan Nb iaitu $1.78 \times 10^{-3} \text{ S cm}^{-1}$ pada 600 °C. Tenaga pengaktifan untuk bahan-bahan telah dianggarkan dalam julat 1.35 - 1.49 eV.

Dopan kation divalensi yang terpilih telah didopkan secara kaedah kimia ke dalam fasa $\beta\text{-Li}_3\text{TaO}_4$. Kedua-dua Mg dan Zn membentuk larutan pepejal terhad dengan nilai $x = 0.1$ sahaja. Formula kimia, $\text{Li}_{3-2x}\text{M}_x\text{TaO}_4$ ($M = \text{Mg}$ or Zn) telah dicadangkan di mana dua Li^+ telah digantikan dengan M^{2+} kation. Kedua-dua bahan terdop telah menunjukkan kekonduksian yang lebih tinggi dari induk $\beta\text{-Li}_3\text{TaO}_4$. Ini mungkin disebabkan oleh kekosongan litium ataupun butiran yang rapat. Kekonduksian yang diperolehi oleh $\text{Li}_{2.8}\text{Mg}_{0.1}\text{TaO}_4$ dan $\text{Li}_{2.8}\text{Zn}_{0.1}\text{TaO}_4$ ialah $3.60 \times 10^{-4} \text{ S cm}^{-1}$ dan $5.99 \times 10^{-4} \text{ S cm}^{-1}$ pada 600 °C. Tenaga pengaktifan yang terhasil tidak menunjukkan sebarang perbezaan yang ketara dan kekal rendah iaitu 0.55 -0.58 eV.

Semua sampel yang telah dihasilkan menunjukkan kestabilan terma kerana tiada kejadian terma ditemui di dalam kedua-dua termogram TGA dan DTA. Stoikiometri kimia untuk sampel ini ditentukan oleh ICP-OES, di mana nilai kepekatan diantara teori dan eksperimen yang diperolehi adalah hampir sama. Analisis struktur oleh FT-IR menemui beberapa ikatan logam-oksigen di dalam julat nombor gelombang 250-1000 cm^{-1} . Bijirin berbentuk tidak teratur ditentukan dalam julat 0.95 -10.82 μm ditentukan dengan menggunakan mikrograp SEM. Ini disokong lagi dengan analisis TEM kerana keputusan menunjukkan zarah sfera bersama segi empat telah ditentukan di dalam sampel.

Dalam usaha untuk menyiasat kemungkinan pembentukan larutan pepejal yang baru dan menentukan prestasi elektrik keatas bahan-bahan $\text{Li}_2\text{O-Ta}_2\text{O}_5$, pendopan kimia telah dijalankan. Bahan-bahan ini menunjukkan had larutan pepejal yang berbeza dan kekonduksian ionik litium yang sederhana.

ACKNOWLEDGEMENTS

In the name of Allah, the Most Gracious and the Most Merciful. Alhamdulillah, all praises to Allah for the Strengths and His blessing in completing this thesis.

Special appreciation goes to my supervisor, Associate Professor Dr. Tan Kar Ban for the continuous support, unfailing helps, invaluable advised and patient throughout of this project. I would like to extend my sincere appreciation to Dr. Khaw Chwin Chieh, Prof. Dr. Zulkarnain Zainal, and Dr. Tan Yen Ping for their insightful comment and suggestions regarding this research work.

I would like to thank to the staff of the Chemistry Department of Chemistry, UPM especially Madam Zaidina and Madam Gina (TGA/DTA), Madam Rusnani Amirudin (FT-IR), Madam Nurhidayu Jamaludin and Madam Siti Fairous (ICP-OES) for their technical assistance, guidance in operating the instruments and data collection. My appreciation also goes to all staff in Electron Microscopy unit, UPM.

My deepest appreciation goes to my beloved parents; Mr. Shari Hanafiah and Mrs. Engsun Said and also to my sister and brothers for their prayer, continuous support and encouragement during my study. Not to be forgotten is my husband, Ahmad Yasir Md Yamin for his love and moral support, joy, and laughter all the way through. Thanks you for always being there.

I would like to thank my lab seniors, Dr Tan Phei Yei, Dr. Chon Mun Ping, Miss Siew Ling and Mr Mohd Khaizarul Hanafi for all their guidance and patience. Not to be forgotten to all my fellow labmates are Miss Kartika Firman, Miss Nurul Aidayu Mat Dasin, Miss Syazmimi Mohd Razi, and Miss Rohayu Md Noor for their kindness and continuous support. I also wish to thank to my roommate Nur Hidayah Mohd Hapipi for the endless support and concerns. Finally, the financial support from the Ministry of Higher Education, Malaysia (MOHE) via Fundamental Research Grant Scheme (FRGS) is gratefully acknowledged.

The thesis was submitted to the Senate of Universiti Putra Malaysia and has been accepted as fulfillment of the requirement for the degree of Master of Science. The members of the Supervisory Committee were Follows:

Tan Kar Ban, PhD
Associate Professor
Faculty of science
Universiti Putra Malaysia
(Chairperson)

Zulkarnain Zainal, PhD
Professor
Faculty of science
Universiti Putra Malaysia
(Member)

Khaw Chwin Chieh, PhD
Lecturer
Lee Kong Chian Faculty of Engineering and Science
Universiti Tunku Abdul Rahman
(Member)

ROBIAH BINTI YUNUS, PhD
Professor and Deputy Dean
School of Graduate Studies
Universiti Putra Malaysia

Date:

Declaration by graduate student

I hereby confirm that:

- this thesis is my original work;
- quotations, illustrations and citations have been duly referenced;
- this thesis has not been submitted previously or concurrently for any other degree at any other institutions;
- intellectual property from the thesis and copyright of thesis are fully-owned by Universiti Putra Malaysia, as according to the Universiti Putra Malaysia (Research) Rules 2012;
- written permission must be obtained from supervisor and the office of Deputy Vice-Chancellor (Research and Innovation) before thesis is published (in the form of written, printed or in electronic form) including books, journals, modules, proceedings, popular writings, seminar papers, manuscripts, posters, reports, lecture notes, learning modules or any other materials as stated in the Universiti Putra Malaysia (Research) Rules 2012;
- there is no plagiarism or data falsification/fabrication in the thesis, and scholarly integrity is upheld as according to the Universiti Putra Malaysia (Graduate Studies) Rules 2003 (Revision 2012-2013) and the Universiti Putra Malaysia (Research) Rules 2012. The thesis has undergone plagiarism detection software.

Signature: _____

Date: _____

Name and Matric No.: Syafiqah binti Shari (GS41167)

Declaration by Members of Supervisory Committee

This is to confirm that:

- the research conducted and the writing of this thesis was under our supervision;
- supervision responsibilities as stated in the Universiti Putra Malaysia (Graduate Studies) Rules 2003 (Revision 2012-2013) are adhered to.

Signature : _____
Name of Chairman of : _____
Supervisory Committee Dr. Tan Kar Ban

Signature : _____
Name of Member of : _____
Supervisory Committee Prof. Dr. Zulkarnain Zainal

Signature : _____
Name of Member of : _____
Supervisory Committee Dr. Khaw Chwin Chieh

TABLE OF CONTENTS

	Page
ABSTRACT	i
ABSTRAK	iii
ACKNOWLEDGEMENTS	v
APPROVAL	vi
DECLARATION	viii
LIST OF TABLES	xii
LIST OF FIGURES	xiv
LIST OF ABBREVIATIONS	xix
CHAPTER	
1. INTRODUCTION	1
1.1. Electroceramics	2
1.2. Solid solution	3
1.3. Ionic conductivity and solid electrolytes	3
1.3.1. Ionic conductors	3
1.4. Application of ionic conductor	5
1.5. Problem statement	6
1.6. Objectives	6
2. LITERATURE REVIEW	7
2.1 Lithium ionic conductivity	7
2.2 Lithium based binary system	8
2.2.1 $\text{Li}_2\text{O} - \text{Nb}_2\text{O}_5$ binary systems	8
2.2.2 $\text{Li}_2\text{O} - \text{Ta}_2\text{O}_5$ binary systems	11
2.3 Li_3TaO_4 and its properties	14
2.4 Introduction of dopants on $\text{Li}_2\text{O}-\text{M}_2\text{O}_5$ (M = Ta or Nb) and related materials	19
2.4.1 Doped $\text{Li}_2\text{O}-\text{Ta}_2\text{O}_5$	19
2.4.2 Doped $\text{Li}_2\text{O}-\text{Nb}_2\text{O}_5$	21
2.5 Related phases	23
3. MATERIALS AND METHODS	24
3.1. Sample preparation	24
3.1.1. Solid state method	24
3.1.2. Sample synthesis	24
3.1.3. Chemical doping	25
3.2. Pellet preparation	25
3.3. Analysis and Characterisations	25
3.3.1. X-ray Diffraction (XRD)	26
3.3.2. Elemental Analysis	28
3.3.2.1. Inductively Coupled Plasma Optical Emission Spectrometry (ICP-OES)	28
3.3.3. Structural analysis	29
3.3.3.1. Fourier-Transform Infrared Spectroscopy (FT-IR)	29

3.3.4. Thermal Analysis	29
3.3.4.1. Thermogravimetric Analysis (TGA)	30
3.3.4.2. Differential Thermal Analysis (DTA)	30
3.3.5. Surface morphology analysis	31
3.3.5.1. Scanning Electron Microscopy (SEM)	31
3.3.5.2. Transmission Electron Microscopy (TEM)	31
3.3.6. Electrical Properties	32
3.3.6.1. Ac impedance spectroscopy	32
3.3.6.2. Cole-Cole plot	33
3.3.6.3. Modulus spectroscopy	36
3.3.6.4. Experiment procedure	37
4. RESULT AND DISCUSSION	38
4.1 Phase formation of $\text{Li}_{3+5x}\text{Ta}_{1-x}\text{O}_4$ solid solution	38
4.1.1 X-ray Diffraction (XRD) analysis	38
4.1.2 Elemental Analysis and Structural Analysis Li_3TaO_4 solid solution	42
4.1.3 Thermal Analysis of Li_3TaO_4 solid solution	43
4.1.4 Crystallite Size and Morphology Studied	46
4.1.5 Electrical properties of Li_3TaO_4 solid solution	53
4.2 Phase formation of $\text{Li}_3\text{Ta}_{1-x}\text{Ti}_x\text{O}_{4-x}$ solid solution	59
4.2.1 X-ray Diffraction (XRD) analysis	59
4.2.2 Elemental Analysis and Structural Analysis $\text{Li}_3\text{Ta}_{1-x}\text{Ti}_x\text{O}_{4-x}$ solid solution	63
4.2.3 Thermal Analysis of $\text{Li}_3\text{Ta}_{1-x}\text{Ti}_x\text{O}_{4-x}$ solid solution	64
4.2.4 Crystallite Size and Morphology Studied	67
4.2.5 Electrical properties of $\text{Li}_3\text{Ta}_{1-x}\text{Ti}_x\text{O}_{4-x}$ solid solution	72
4.3 Phase formation of $\text{Li}_3\text{Ta}_{0.5-x}\text{Nb}_x\text{Ti}_{0.5}\text{O}_{3.75}$ solid solution	78
4.3.1 X-ray Diffraction (XRD) analysis	78
4.3.2 Elemental Analysis and Structural Analysis $\text{Li}_3\text{Ta}_{0.5-x}\text{Nb}_x\text{Ti}_{0.5}\text{O}_{3.75}$ solid solution	80
4.3.3 Thermal Analysis of $\text{Li}_3\text{Ta}_{0.5-x}\text{Nb}_x\text{Ti}_{0.5}\text{O}_{3.75}$ solid solution	82
4.3.4 Crystallite Size and Morphology Studied	84
4.3.5 Electrical properties of $\text{Li}_3\text{Ta}_{0.5-x}\text{Nb}_x\text{Ti}_{0.5}\text{O}_{3.75}$ solid solution	90
4.4 Phase formation of $\text{Li}_{3-2x}\text{M}_x\text{TaO}_4$ (M = Mg, Zn)	96
4.4.1 X-ray Diffraction (XRD) analysis	96
4.4.2 Elemental and Structural Analysis $\text{Li}_{3-2x}\text{M}_x\text{TaO}_4$	99
4.4.3 Thermal Analysis of $\text{Li}_{3-2x}\text{M}_x\text{TaO}_4$	101
4.4.4 Crystallite Size and Morphology Studied	101
4.4.5 Electrical properties of $\text{Li}_{3-2x}\text{M}_x\text{TaO}_4$	105
5. CONCLUSIONS	111
FURTHER WORK	113
REFERENCES	114
APPENDICES	124
BIODATA OF STUDENT	158

LIST OF TABLES

Table	Page
1.1 Electrical microstructure of electroceramics	1
1.2 Typical values of electrical conductivity of ionic and electronic materials	4
2.1 Phase composition of $\text{Li}_2\text{O} - \text{Nb}_2\text{O}_5$ systems	8
2.2 Summary of activation energy, (E_a) values and pre-exponential factor, (σ_0) of $\text{Li}_{1-x}\text{Nb}_{1+x/5}\text{O}_3$ ($0.0025 \leq x \leq 0.075$)	10
2.3 Summary of the phase composition of $\text{Li}_2\text{O} - \text{Ta}_2\text{O}_5$ binary systems	15
3.1 The absorption wavelengths used for ICP-OES chemical analysis	29
3.2 Summary of capacitance values with their respective phenomenon	35
4.1 The lattice parameters of $\text{Li}_{3+5x}\text{Ta}_{1-x}\text{O}_4$ ($0 \leq x \leq 0.059$) solid solution	41
4.2 Elemental concentration analyses of $\text{Li}_{3+5x}\text{Ta}_{1-x}\text{O}_4$ solid solution	42
4.3 Fourier transforms infrared spectra of $\text{Li}_{3+5x}\text{Ta}_{1-x}\text{O}_4$ solid solution	43
4.4 Summary of crystallite sizes, internal strain and grain size of $\text{Li}_{3+5x}\text{Ta}_{1-x}\text{O}_4$ solid solution	48
4.5 Summary of the ionic conductivity, σ and activation energy, E_a of $\text{Li}_{3+5x}\text{Ta}_{1-x}\text{O}_4$ solid solution at 250 °C and 300 °C	57
4.6 Summary of phases present and synthesis conditions in the $\text{Li}_3\text{Ta}_{1-x}\text{Ti}_x\text{O}_{4-x/2}$ ($0 \leq x \leq 0.80$) system	61
4.7 Lattice parameters and cell volumes of $\text{Li}_3\text{Ta}_{1-x}\text{Ti}_x\text{O}_{4-x/2}$ ($0.45 \leq x \leq 0.75$) solid solution	63
4.8 Elemental analysis of $\text{Li}_3\text{Ta}_{1-x}\text{Ti}_x\text{O}_{4-x/2}$ ($x = 0; 0.45 \leq x \leq 0.75$) solid solutions	64
4.9 The Fourier transforms infrared spectra of $\text{Li}_3\text{Ta}_{1-x}\text{Ti}_x\text{O}_{4-x/2}$ ($x = 0; 0.45 \leq x \leq 0.75$)	65
4.10 Crystallite sizes and internal strains of $\text{Li}_3\text{Ta}_{1-x}\text{Ti}_x\text{O}_{4-x/2}$ ($x = 0; 0.45 \leq x \leq 0.75$) solid solution by Scherrer and W-H methods	67
4.11 Conductivity values for $\text{Li}_3\text{Ta}_{1-x}\text{Ti}_x\text{O}_{4-x/2}$ ($x = 0; 0 \leq x \leq 0.75$) at different temperatures	76

4.12	Elemental analysis of $\text{Li}_3\text{Ta}_{0.5-x}\text{Nb}_x\text{Ti}_{0.5}\text{O}_{3.75}$ solid solution	81
4.13	The Fourier transforms infrared spectra of $\text{Li}_3\text{Ta}_{0.5-x}\text{Nb}_x\text{Ti}_{0.5}\text{O}_{3.75}$ solid solution ($0 \leq x \leq 0.5$)	81
4.14	Crystallite sizes and internal strains of $\text{Li}_3\text{Ta}_{0.5-x}\text{Nb}_x\text{Ti}_{0.5}\text{O}_{3.75}$ ($0 \leq x \leq 0.5$) solid solutions by Scherrer and W-H methods	85
4.15	Summary of the resistivities, R_b and conductivities, σ of $\text{Li}_3\text{Ta}_{0.5-x}\text{Nb}_x\text{Ti}_{0.5}\text{O}_{3.75}$ and $\text{LiTa}_{1-x}\text{Nb}_x\text{O}_3$ solid solutions at 800°C	91
4.16	Conductivity values of $\text{Li}_3\text{Ta}_{0.5-x}\text{Nb}_x\text{Ti}_{0.5}\text{O}_{3.75}$ ($0 \leq x \leq 0.5$) at different temperatures	95
4.17	Lattice parameters of Li_3TaO_4 , $\text{Li}_{2.8}\text{Mg}_{0.1}\text{TaO}_4$ and $\text{Li}_{2.8}\text{Zn}_{0.1}\text{TaO}_4$	99
4.18	Elemental analysis of Li_3TaO_4 , $\text{Li}_{2.8}\text{Mg}_{0.1}\text{TaO}_4$ and $\text{Li}_{2.8}\text{Zn}_{0.1}\text{TaO}_4$	100
4.19	The Fourier transforms infrared spectra of Li_3TaO_4 , $\text{Li}_{2.8}\text{Mg}_{0.1}\text{TaO}_4$ and $\text{Li}_{2.8}\text{Zn}_{0.1}\text{TaO}_4$	100
4.20	Calculated crystallite sizes and strains of Li_3TaO_4 , $\text{Li}_{2.8}\text{Mg}_{0.1}\text{TaO}_4$ and $\text{Li}_{2.8}\text{Zn}_{0.1}\text{TaO}_4$	103
4.21	Summary of conductivity values of Li_3TaO_4 , $\text{Li}_{2.8}\text{Mg}_{0.1}\text{TaO}_4$ and $\text{Li}_{2.8}\text{Zn}_{0.1}\text{TaO}_4$ at different temperatures	109

LIST OF FIGURES

Figure		Page
1.1	Solid electrolytes as intermediate between normal crystalline solids and liquids	3
2.1	A view of Nb_4O_{16} cluster and a Li ion with coordinating O^{2-} . Filled, dotted and open circles represents Nb^{5+} , Li^+ and O^{2-} ion, respectively	9
2.2	Phase diagram of Li_2O - Nb_2O_5 binary systems	11
2.3	Phase diagram for the Ta_2O_5 – Li_2O system. The thin dashed line represents the metastable equilibrium between Ta_2O_5 and LiTaO_3 in the absence of LiTa_3O_8	12
2.4	Monoclinic structure of $\beta\text{-Li}_3\text{TaO}_4$, emphasizing edge-sharing TaO_6 octahedra. Li atoms are shown as white circles	17
2.5	Cation order adopted by Li (white circles) and Ta (black circles) between cp oxygen layers in $\beta\text{-Li}_3\text{TaO}_4$	17
2.6	Crystal structure of $\alpha\text{-Li}_3\text{TaO}_4$ showing TaO_6 octahedra; Li atoms (white circle)	18
2.7	Cation order adopted by Li (white circles) and Ta (black circles) between close packed oxygen layers layers in $\alpha\text{-Li}_3\text{TaO}_4$	18
3.1	Flow chart for sample preparation and characterization	26
3.2	The X-ray diffraction experiment	27
3.3	Principle of x-ray diffraction	27
3.4	Complex impedance plots and equivalent circuit proposed for materials exhibiting bulk; ionic conduction with blocking electrode	34
3.5	Brickwork model of grain and grain boundary region in a ceramic placed between metal electrodes	35
3.6	Infinite, Warburg-type ionic diffusion with an associated charge transfer element R_2C_2	36
3.7(a)	A complex Z^* plot	37
3.7(b)	Z'' and M'' spectroscopy plots	37

4.1	Phase evolution of β - Li_3TaO_4 in the temperature range 600 °C - 925 °C	39
4.2	XRD patterns of the prepared $\text{Li}_{3+5x}\text{Ta}_{1-x}\text{O}_4$ ($0 \leq x \leq 0.059$) solid solution; LiTaO_3 (\blacktriangle) and $\text{Li}_8\text{Ta}_2\text{O}_9$ (\blacksquare)	40
4.3	Variation of lattice parameters (a, b and c) as a function of composition in $\text{Li}_{3+5x}\text{Ta}_{1-x}\text{O}_4$ ($0 \leq x \leq 0.059$)	41
4.4	FTIR spectra of $\text{Li}_{3+5x}\text{Ta}_{1-x}\text{O}_4$ solid solution ($0 \leq x \leq 0.059$)	43
4.5(a)	TGA thermogram of Li_2CO_3 - Ta_2O_5 and Li_3TaO_4	44
4.5(b)	TGA thermogram of calcined $\text{Li}_{3+5x}\text{Ta}_{1-x}\text{O}_4$ ($0 \leq x \leq 0.059$) solid solution	45
4.6(a)	DTA thermograms of Li_2CO_3 - Ta_2O_5 and Li_3TaO_4	45
4.6(b)	DTA thermograms of $\text{Li}_{3+5x}\text{Ta}_{1-x}\text{O}_4$ solid solution ($0 \leq x \leq 0.059$)	46
4.7	Williamson-Hall plots of $\text{Li}_{3+5x}\text{Ta}_{1-x}\text{O}_4$ solid solution	47
4.8	Comparison between crystallite sizes calculated by Scherrer and Williamson-Hall method, and the internal strain of $\text{Li}_{3+5x}\text{Ta}_{1-x}\text{O}_4$ solid solution as a function of x	48
4.9	SEM micrographs (Left) and the grain size distribution (Right) of $\text{Li}_{3+5x}\text{Ta}_{1-x}\text{O}_4$ solid solution at 5 k magnification	49
4.10	Grain sizes and densities of pellet $\text{Li}_{3+5x}\text{Ta}_{1-x}\text{O}_4$ solid solution as a function of x	51
4.11	TEM micrographs of $\text{Li}_{3+5x}\text{Ta}_{1-x}\text{O}_4$ ($0 \leq x \leq 0.059$) solid solution captured at 100 nm magnification	52
4.12	Complex Cole-Cole plots of Li_3TaO_4 at 200 °C, 250 °C and 300 °C	54
4.13	Complex Cole-Cole plots of Li_3TaO_4 at 500 °C, 550 °C and 601 °C	55
4.14	Complex Cole-Cole plots of $\text{Li}_{3+5x}\text{Ta}_{1-x}\text{O}_4$ solid solution at 350 °C	55
4.15	A combined spectroscopic plots of Z'' and M'' of Li_3TaO_4 as a function of frequency at 300 °C	56
4.16	The conductivity Arrhenius plots of the $\text{Li}_{3+5x}\text{Ta}_{1-x}\text{O}_4$ ($0 \leq x \leq 0.059$) samples	58

4.17	XRD patterns of $\text{Li}_3\text{Ta}_{1-x}\text{Ti}_x\text{O}_{4-x/2}$ ($0 \leq x \leq 0.45$) sintered at 925 °C for 24 h	60
4.18	XRD patterns of $\text{Li}_3\text{Ta}_{1-x}\text{Ti}_x\text{O}_{4-x/2}$ ($0.45 \leq x \leq 0.80$) sintered at 925 °C for 24 h.	60
4.19	Constant shift of (0 2 0) diffraction plane of $\text{Li}_3\text{Ta}_{1-x}\text{Ti}_x\text{O}_{4-x/2}$ ($0.45 \leq x \leq 0.75$) solid solutions	62
4.20	Variation of lattice parameters as a function of x in $\text{Li}_3\text{Ta}_{1-x}\text{Ti}_x\text{O}_{4-x/2}$ ($0.45 \leq x \leq 0.75$) solid solution	62
4.21	IR spectra of $\text{Li}_3\text{Ta}_{1-x}\text{Ti}_x\text{O}_{4-x/2}$ ($x = 0; 0.45 \leq x \leq 0.7$)	65
4.22	TGA thermograms of $\text{Li}_3\text{Ta}_{1-x}\text{Ti}_x\text{O}_{4-x/2}$ ($x = 0; 0.45 \leq x \leq 0.75$) solid solution	66
4.23	DTA thermograms of $\text{Li}_3\text{Ta}_{1-x}\text{Ti}_x\text{O}_{4-x/2}$ ($x = 0; 0.45 \leq x \leq 0.75$) solid solution	66
4.24	Williamson-Hall plots of $\text{Li}_3\text{Ta}_{1-x}\text{Ti}_x\text{O}_{4-x/2}$ solid solution ($0.45 \leq x \leq 0.75$)	68
4.25	Comparison between crystallites sizes, D calculated by Sherrer and W-H methods, and the internal strains of $\text{Li}_3\text{Ta}_{1-x}\text{Ti}_x\text{O}_{4-x/2}$ solid solution ($0.45 \leq x \leq 0.75$)	68
4.26	SEM micrographs (Left) and histograms of the grain size distribution of $\text{Li}_3\text{Ta}_{1-x}\text{Ti}_x\text{O}_{4-x/2}$ ($x = 0; 0.45 \leq x \leq 0.75$) solid solution captured at magnification of 5k	69
4.27	TEM micrographs of $\text{Li}_3\text{Ta}_{1-x}\text{Ti}_x\text{O}_{4-x/2}$ ($x = 0; 0.45 \leq x \leq 0.75$) solid solution captured at 50 nm magnification	71
4.28	Complex Cole-Cole plots of $\text{Li}_3\text{Ta}_{1-x}\text{Ti}_x\text{O}_{4-x/2}$ ($x = 0; 0.45 \leq x \leq 0.75$) solid solution at temperature 550 °C	74
4.29	Cole-Cole plots of $\text{Li}_3\text{Ta}_{0.25}\text{Ti}_{0.75}\text{O}_{3.625}$ measured at different temperatures	74
4.30	Real admittance plots, Y' of $\text{Li}_3\text{Ta}_{0.25}\text{Ti}_{0.75}\text{O}_{3.625}$ as a function of frequency at various temperatures	75
4.31	Combined Z'' and M'' spectroscopic plots of $\text{Li}_3\text{Ta}_{0.55}\text{Ti}_{0.45}\text{O}_{3.725}$ at ~500 °C	75
4.32	Arrhenius plots of Ti-doped materials with general formula $\text{Li}_3\text{Ta}_{1-x}\text{Ti}_x\text{O}_{4-x/2}$ ($0.45 \leq x \leq 0.75$) solid solution	77

4.33	XRD patterns of $\text{Li}_3\text{Ta}_{0.5-x}\text{Nb}_x\text{Ti}_{0.5}\text{O}_{3.75}$ ($0 \leq x \leq 0.5$) solid solution	79
4.34	Variation of lattice parameters as a function of x in $\text{Li}_3\text{Ta}_{0.5-x}\text{Nb}_x\text{Ti}_{0.5}\text{O}_{3.75}$ ($0 \leq x \leq 0.5$) solid solution	80
4.35	IR spectra of $\text{Li}_3\text{Ta}_{0.5-x}\text{Nb}_x\text{Ti}_{0.5}\text{O}_{3.75}$ solid solution	82
4.36	TGA thermograms of $\text{Li}_3\text{Ta}_{0.5-x}\text{Nb}_x\text{Ti}_{0.5}\text{O}_{3.75}$ solid solution	83
4.37	DTA thermograms of $\text{Li}_3\text{Ta}_{0.5-x}\text{Nb}_x\text{Ti}_{0.5}\text{O}_{3.75}$ solid solution	83
4.38	Williamson-Hall plots of $\text{Li}_3\text{Ta}_{0.5-x}\text{Nb}_x\text{Ti}_{0.5}\text{O}_{3.75}$ solid solution ($0 \leq x \leq 0.5$)	84
4.39	Comparison between crystallites sizes, D calculated by Sherrer and W-H methods, and the internal strains of $\text{Li}_3\text{Ta}_{0.5-x}\text{Nb}_x\text{Ti}_{0.5}\text{O}_{3.75}$ solid solution ($0 \leq x \leq 0.5$)	85
4.40	SEM micrographs (Left) and histograms of the grain size distribution (Right) of $\text{Li}_3\text{Ta}_{0.5-x}\text{Nb}_x\text{Ti}_{0.5}\text{O}_{3.75}$ ($0 \leq x \leq 0.5$) captured at 5k magnification	86
4.41	Distribution of grain size versus composition, x of $\text{Li}_3\text{Ta}_{0.5-x}\text{Nb}_x\text{Ti}_{0.5}\text{O}_{3.75}$ ($0 \leq x \leq 0.5$)	88
4.42	TEM micrographs of $\text{Li}_3\text{Ta}_{0.5-x}\text{Nb}_x\text{Ti}_{0.5}\text{O}_{3.75}$ ($0 \leq x \leq 0.5$) solid solution captured at 50 nm magnification	89
4.43	Complex impedance plane plots for $\text{Li}_3\text{Ta}_{0.5-x}\text{Nb}_x\text{Ti}_{0.5}\text{O}_{3.75}$ solid solution at temperature 550 °C	92
4.44	Complex Cole-Cole plot of $\text{Li}_3\text{Ta}_{0.4}\text{Nb}_{0.1}\text{Ti}_{0.5}\text{O}_{3.75}$ at 450 °C and 599 °C	92
4.45	Real admittance, Y' plot of $\text{Li}_3\text{Ta}_{0.4}\text{Nb}_{0.1}\text{Ti}_{0.5}\text{O}_{3.75}$ as a function of frequency at various temperatures	93
4.46	Combined Z'' and M'' spectroscopic plots of $\text{Li}_3\text{Ta}_{0.4}\text{Nb}_{0.1}\text{Ti}_{0.5}\text{O}_{3.75}$ at 450 °C	94
4.47	Conductivity Arrhenius plots of $\text{Li}_3\text{Ta}_{0.5-x}\text{Nb}_x\text{Ti}_{0.5}\text{O}_{3.75}$ solid solution	95
4.48	XRD patterns for unsuccessful of $\text{Li}_{3-2x}\text{M}_x\text{TaO}_4$ (M = Ca, Sr, Ba, Ni, Pb) at 925 °C for 48 h	97
4.49	XRD patterns of $\text{Li}_{3-2x}\text{Mg}_x\text{TaO}_4$ ($0 \leq x \leq 0.2$) at 925 °C	98
4.50	XRD patterns of $\text{Li}_{3-2x}\text{Zn}_x\text{TaO}_4$ ($0 \leq x \leq 0.2$) at 925 °C	98

4.51	Variation of lattice parameters of Li_3TaO_4 , $\text{Li}_{2.8}\text{Mg}_{0.1}\text{TaO}_4$ and $\text{Li}_{2.8}\text{Zn}_{0.1}\text{TaO}_4$	99
4.52	IR spectra of Li_3TaO_4 , $\text{Li}_{2.8}\text{Mg}_{0.1}\text{TaO}_4$ and $\text{Li}_{2.8}\text{Zn}_{0.1}\text{TaO}_4$	101
4.53	TGA thermogram of Li_3TaO_4 , $\text{Li}_{2.8}\text{Mg}_{0.1}\text{TaO}_4$ and $\text{Li}_{2.8}\text{Zn}_{0.1}\text{TaO}_4$.	102
4.54	DTA thermograms of Li_3TaO_4 , $\text{Li}_{2.8}\text{Mg}_{0.1}\text{TaO}_4$ and $\text{Li}_{2.8}\text{Zn}_{0.1}\text{TaO}_4$	102
4.55	Williamson-Hall plots of Li_3TaO_4 , $\text{Li}_{2.8}\text{Mg}_{0.1}\text{TaO}_4$ and $\text{Li}_{2.8}\text{Zn}_{0.1}\text{TaO}_4$	103
4.56	SEM micrographs (Left) and histograms of the grain size distribution (Right) of Li_3TaO_4 , $\text{Li}_{2.8}\text{Mg}_{0.1}\text{TaO}_4$ and $\text{Li}_{2.8}\text{Zn}_{0.1}\text{TaO}_4$	104
4.57	Complex Cole-Cole plots of Li_3TaO_4 , $\text{Li}_{2.8}\text{Mg}_{0.1}\text{TaO}_4$ and $\text{Li}_{2.8}\text{Zn}_{0.1}\text{TaO}_4$ at 350 °C	106
4.58	Cole-Cole plots of $\text{Li}_{2.8}\text{Zn}_{0.1}\text{TaO}_4$ at different temperatures	107
4.59	Combined spectroscopic plots of Z'' and M'' of $\text{Li}_{2.8}\text{Zn}_{0.1}\text{TaO}_4$ as a function of frequency at temperature of 303 °C	108
4.60	Real admittance, Y' plot of the $\text{Li}_{2.8}\text{Zn}_{0.1}\text{TaO}_4$ as a function of frequency at various temperatures	109
4.61	Arrhenius plots of the bulk conductivity for the Li_3TaO_4 , $\text{Li}_{2.8}\text{Mg}_{0.1}\text{TaO}_4$ and $\text{Li}_{2.8}\text{Zn}_{0.1}$	110

LIST OF ABBREVIATIONS / NOTATIONS / GLOSSARY OF TERMS

3D	Three dimensions
ac	Alternating current
DTA	differential thermal analysis
FT-IR	Fourier-transform infrared
ICDD	international centre for diffraction data
ICP-AES	inductively-coupled plasma-atomic emission spectrometry
JCPDS	Joint Committee on Powder Diffraction standards
SEM	scanning electron microscopy
TEM	transmission electron microscopy
TGA	thermogravimetry analysis
XRD	X-ray diffraction
A, b, c, α , β , γ	lattice constant
A	area
A_w	Warburg coefficient
C	Capacitance
C_b	Bulk capacitance
C_{dl}	Double-layer capacitance
C_{gb}	Grain boundary capacitance
C_o	Vacuum capacitance
d	d-spacing
D	Density
e	Charge of the conducting species
ϵ_o	Permittivity of free space
E	Electric field
E_o	Activation energy
ϵ'	Relative permittivity
ϵ^*	Complex permittivity
f	Frequency
F	Faraday constant
h, k, l	Miller indice
I	Current
j	Flux of charge
J	Density of the current
τ	Thickness
λ	Wavelength
M	Dopant introduced
M'	Real part of modulus
M''	Imaginary part of modulus
M^*	Complex modulus
μ	Mobility of the species
R	Resistance
R_b	Bulk resistance
R_{gb}	Grain boundary resistance
σ	Bragg angle

τ	Electrical relaxation times
T	temperature
ω	Angular frequency
Z	Formula unit
Z	Impedance
Z'	Real part of impedance
Z''	Imaginary part of impedance
Z^*	Complex impedance



© COPYRIGHT UPM

CHAPTER 1

INTRODUCTION

1.1 Electroceramics

Electroceramics are advanced materials which are used in electrical, optical and magnetic applications (Bharadwaj *et al.*, 2012). This includes several groups of dielectric and conductive ceramics. In general, dielectric ceramics counting a large number of materials which can be divided either linear or non-linear dielectric. On the contrary, conductive ceramics are more numerous, including superconductors, semiconductors and conductors of which the charge carrier could be either ions or electrons (Setter, 2001).

There are two categories of conductive ceramics which are either electrically homogeneous or heterogeneous (Table 1.1). The electrically homogeneous materials, e.g. ionically conducting ceramics or microwave dielectrics, usually have high dense microstructure of which the grain boundaries have less influence on their electrical properties. On the contrary, electrically heterogeneous materials, e.g. varistors and barrier capacitors, have properties which are controlled by the structure of interfacial region at grain boundaries and grain surface. In addition, these materials rely strongly on the control processing control by a series of post-sintering heat treatments, so that the correct defect segregation, degree oxidation or reduction at the grain boundaries and surfaces could be achieved (West *et al.*, 2004).

Ceramic materials have been used in a wide range of industrial applications, e.g. electrical and electronic components, superconductors, catalysts, and automobile components. These materials are generally polycrystalline, which are comprised of inorganic, non-metallic, non-water soluble compounds that show ionic contribution in their chemical bond. Other examples of applications including transportation, industrial production, power engineering, medicine and health care, consumer electronic and communication (Setter and Waser, 2000).

Table 1.1: Electrical microstructure of electroceramics (West *et al.*, 2004)

Electrically homogeneous	Electrically heterogeneous (grain boundary controlled)
Ionic conductors	Varistors
Mixed conductors	Barrier layer capacitors
High T_c superconductors	PTC thermistors
Microwave dielectric	Gas sensors

1.2 Solid Solution

A solid solution is mostly a crystalline material that has variable composition and its properties usually vary with composition. Generally, a simple solid solution could divide into two types either substitutional solid solution or interstitial solid solution. For substitutional solid solution, atoms or ions that replace each other must have the same charge in the parent structure. On the other hand, interstitial solid solution has introduced species that to occupy a site that is normally empty and no ions or atoms are left out in the crystal structure.

Dopants are generally introduced into a host structure in order to enhance the electrical properties (Moulson and Herbert, 2003). Several requirements must be met: first, the ions that replace each other must have the same charge to maintain electroneutrality, else a structural change involving either vacancies or interstitial is required. Second, the replacing ion must be fairly similar in size. For example, the formation of metal alloy would allow 15 % difference in the ionic radii. In the case of extensive solid solution, ions of similar size may substitute each other easily and the resulted solid solution is stable at all temperatures.

On the other hand, doping with aliovalent cations (the replacing and replaceable ion have difference oxidation states) would require creation of vacancies or interstitials (ionic compensation) or electron or holes (electronic compensation). Therefore, substitution of a cation with lower valence may result in either anion (oxide ion) vacancies or interstitial cations. Meanwhile, for substitution by higher valence cations would give interstitial anions and cation vacancies (West, 1999).

In this study, few dopants with different charges have been introduced into host structure in order to investigate the influence of these on doping mechanism and electrical properties. The dopants are chosen, e.g. Mg^{2+} , Zn^{2+} , Ti^{4+} , and Nb^{5+} . The selection of these dopants is mainly based on their chemical and physical properties. These are the determining factors that influence the formation of new solid solution. Divalent cations, Mg^{2+} and Zn^{2+} are expected to form an extensive solid solution due to the factor of charge as the introduction of these dopants may create lithium vacancies for charge compensation, where two Li^+ ions are substituted by one divalent ion. Meanwhile, a tetravalent cation, (e.g. Ti^{4+}) is selected due to the size of ionic radii between the guest and host is less than 15%, therefore the formation of an extensive solid solution may be possible. This Ti^{4+} is used as a dopant for substitution at the Ta-site of $\beta-Li_3TaO_4$. The formation will create more oxygen vacancies for the charge compensation in order to preserve the overall electroneutrality of the system. Lastly, pentavalent cations are chosen due to the replacing ion Nb^{5+} directly replaces the same charge Ta^{5+} ion in the parent structure, thus neither vacancies nor interstitialcies are required to maintain the overall electroneutrality of the system. Furthermore, both Nb^{5+} and Ta^{5+} have an identical ionic radii ($r= 0.64 \text{ \AA}$) at the six coordination, thus the extensive solid solution are expected to form. In this study, the effects of all dopant are determined in term of solid solubility, structural and electrical properties.

1.3 Ionic Conductivity and Solid Electrolytes

The first observation of conductivity in solid electrolytes was more than 150 years ago. Ionic conductivity occurs in materials known as solid electrolytes, superionic conductors or fast ion conductors with ions acting as charge carriers. While, for mixed conduction usually refers to the materials with good electronic conduction. Superionic conductor or fast ion conductor is good for ionic conduction with negligible electronic conductivity (Kumar and Yashonath, 2006).

In solid electrolytes, either cations or anions are free to move throughout the structure, i.e. they are not confined to specific lattice sites. Therefore, solid electrolytes are well known as intermediate between typical ionic solids, all ions are fixed on their lattice sites in a regular 3 dimensional structures. On the contrary, all ions are mobile in liquid electrolyte which does not have a regular structure. Usually solid electrolytes are stable at high temperature, while on cooling may they transform to a polymorph with a low ionic conductivity at low temperatures. The types of crystal structure shown are Figure 1.1.

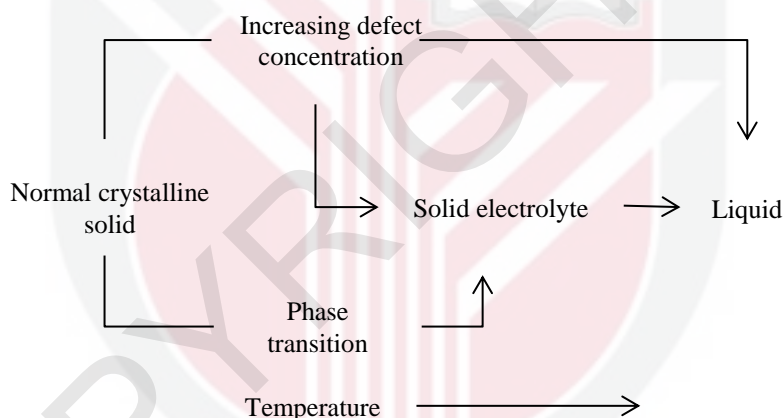


Figure 1.1: Solid electrolytes as intermediate between normal crystalline solids and liquids (West, 1999)

In addition, ionic conductivity is related to the presence of defects or disordered structure that may have a variation of positions by replacement of certain ion in the crystal structure. These materials have a high ionic conductivity can be classified into four groups with thermally induced defects, impurity-induced defects, crystal structure disorder and amorphous character (Koller, 1994).

1.3.1 Ionic Conductors

Solid ionic conductors are generally polycrystalline compounds in which electric current is carried by charged atoms, i.e. by ions. The passage of current is associated with mass transfer and such ionic conductors are called solid electrolytes. Examples of

solid ionic conductor including doped ZrO_2 , AgI , $\beta-Al_2O_3$ and CaF_2 . Ionic conduction in ceramic materials is associated with the movement of ionic point defect, the creation or movement requires energy. The conductivity increases with increasing temperature for all materials except metal and superconductors. Therefore, ceramic solid electrolytes are suitable for high temperature application. (Rickert, 1978; Moulson and Herbert, 2003). The examples of ionic and electronic materials are tabulated in Table 1.2.

Table 1.2: Typical values of electrical conductivity of ionic and electronic materials (West, 1999)

Conduction mechanism	Materials	Conductivity, σ ($ohm^{-1} cm^{-1}$)
Ionic conduction	Ionic crystals	$< 10^{-18} - 10^{-4}$
	Solid electrolytes	$10^{-3} - 10^4$
	Strong (liquid) electrolyte	$10^{-3} - 10^4$
Electronic conduction	Metals	$10^{-1} - 10^5$
	Semiconductors	$10^{-5} - 10^2$
	Insulators	$< 10^{-12}$

In ionic solids, ions are trapped on their lattice sites and they rarely have enough thermal energy to escape from their lattice site but to vibrate continuously. In The process of migration, hopping or diffusion is required, therefore ions must be able to escape and move into adjacent lattice sites. If some sites are vacant, the adjacent ions can hop into these vacancies, thus leaving their own sites vacant or some ions in interstitial sites which can hop into adjacent interstitial sites. Thus, ionic conduction is easier at high temperatures especially ions could vibrate more vigorously and the defect concentrations are higher (West, 1999).

For any material and charge carrier, the specific conductivity, σ proportionality constant between the current density, j and the electric field, E is given by

$$j/E = \sigma = \sum_i n_i e_i \mu_i \quad (1.1)$$

While, for ionic conductivity, σ

$$\sigma = N_{ion} e \mu_{ion} \quad (1.2)$$

Where N_{ion} is the number of ion which can change their position under the influence of electric field, μ_{ion} is the mobility of these ions and e is the elementary charge.

Factors that influence the conductivity are the concentration of charge carrier, temperature, the availability of vacant-accessible sites (which is controlled by the

density of defects in the crystal) and ease of jumping of ions to another site. The numbers of jumping or hopping ions to a neighboring site is controlled by activation energy. The activation energy is a phenomenological quantity as it indicates the free energy barrier an ion has to overcome for a successful jump between the sites. Among the various factors that influence the ionic conductivity of a materials the activation energy is the utmost important factor since its dependence is exponential from Arrhenius expression (Kumar and Yashonath, 2006). The temperature dependence ionic conductivity is usually deduced by using Arrhenius equation, where the graph of $\log_e \sigma$ against $1/T$ should give a straight line with the slope $-E_a/R$.

$$\sigma = A \exp (-E_a/RT) \quad (1.3)$$

Where σ is the conductivity at temperature T in Kelvin, K , R is the Boltzman's constant, E_a is the activation energy and A is called the pre-exponential factor, which depends on the vibration frequency of the potential mobile ions and same structural parameter (West,1999).

1.4 Application of Ionic Conductivity

There are numerous examples of materials with high ionic conductivity in the solid state, e.g. Ag^+ ions in $RbAg_4I_5$, Li^+ ions in α - Li_2SO_4 (> 570 °C) and Na^+ ions in β, β'' -alumina. The high ionic conductivity value are found in the range 10^{-3} - $10^1 \Omega^{-1} cm^{-1}$ with activation energies in the range 0.1-0.3 eV (Lee and West, 1991). The applications of solid electrolytes in electrochemical devices have several advantages and this includes a long life, high energy density etc. Therefore, there are suitable for compact power batteries used in pace-maker, mobile telephones, laptops etc. Besides, they are can used to study thermodynamics and kinetics problems, and to build fuel cell, batteries, sensors and chemotronic components (Rickert, 1978).

In addition, ionic conduction material is also found in sodium-sulfur cell. The cell systems have been developed with other solid electrolytes, some of these being characterised by very long lifetime. The storage time is more than ten years, whose lifetime cannot be even approached with conversional batteries. Rickert (1978) found that the energy density of the sodium-sulfur cell is much greater than the customary lead accumulators. Moreover, the cell can be recharged by reversing the direction of the current. These reasons present the great interest in this sodium-sulfur cell for large-scale energy storage and for electric motor vehicles well known as electrotraction.

Ionic conducting ceramic such as cubic ZrO_2 which has heavily doped acceptor, are used for electrochemical oxygen sensors in car and for high-temperature solid oxide fuel cells (SOFCs). In addition, SOFC could produce electricity directly from oxidising a fuel. It is about 2-3 times more efficient if compared to a thermal engine as SOFC converts chemical potential to the electrical energy. By, reversing the current flow this can induce the full cell to be an electrolyser and energy storage (Setter and Waser, 2000).

In 1972, a cardiac pacemaker was first implanted into a human, which was powered by Li/I₂. Lithium/iodine pacemaker battery worked even though the electrolytes have a low conductivity 10⁻⁷ S/cm at room temperature. The battery was suitable as the application required an isothermal operation at 37 °C, at a very low rate (10-year rate). The cell was a Wilson Greatbatch Model 702/C. To date, there are several million persons have benefited from these implantable devices (Ginnings *et al.*, 1930; Owens *et al.*, 1986).

1.5 Problem Statement

Intensive research has been focused on the materials of LiTaO₃ and LiNbO₃ systems due to their interesting optical properties. However, a structurally related β-Li₃TaO₄ has received less attention and limited information is available in literature review specifically about the structural and electrical properties. Few reported compositions may have been a mixture that contain trace amount of other secondary phases. Besides that, the study concerning chemical doping of the β-Li₃TaO₄ is rarely reported. Therefore, this research is undertaken to study the formation mechanism and to determine the optimised synthesis condition for the sample preparation. The effect of chemical doping on the electrical properties is also part of the investigation. Hence, the correlation between composition and the electrical properties of various phases and other related solid solution in the Li₂O – Ta₂O₅ systems has been discussed systematically.

1.6 Objectives

The objectives of this research are:

1. To synthesise β-Li₃TaO₄ phase and other new related phases in the Li₂O-Ta₂O₅ system.
2. To study the thermal stability, structure and subsolidus solution of the prepared samples.
3. To investigate the effect of chemical dopants, e.g. TiO₂, Nb₂O₅, MgO and ZnO in the Li₂O-Ta₂O₅ system as to explore the possibility of new solid solution formation and determine their electrical performance by using ac impedance spectroscopy.

REFERENCES

- Abbattista, F., Vallino, M. and Mazza, D. 1987. Remark on the binary systems LiO-Me₂O₅ (Me= Nb, Ta). *Journal of Materials Research Bulletin*. 22:1019–1027.
- Allemann, J. A., Xia, Y., Morriss, R. E., Wilkinson, A. P., Eckert, H., Speck, J. S. and Lange, F. F. 1996. Crystallization behavior of Li_{1-5x}Ta_{1+x}O₃ glasses synthesized from liquid precursors. *Journal of Materials Research*. 11: 2379–2387.
- Arnold Reisman. 1961. “Compound Repetition in Oxide Systems, Solid Phases in the System Li₂O-Ta₂O₅ and Na₂O-Ta₂O₅.” *Journal physics chemistry* 66: 15.
- Almond, D.P. and West. A.R. 1983. Impedance modulus spectroscopy of Real dispersive conductors. *Journal of Solid State*. 11:64-75.
- Bae, S. I., Ichikawa, J., Shimamura, K., Onodera, H. and Fukuda, T. 1997. Doping effects of Mg and/or Fe ions on congruent LiNbO₃ single crystal growth. *Journal of Crystal Growth*. 180: 94–100.
- Bak, K. Y., Tan, K. B., Khaw, C. C., Zainal, Z., Tan, P. Y., and Chon, M. P. 2014. Structural and Electrical Properties of Nb-substituted LiTa_{1-x}Nb_xO₃. *Journal of Sains Malaysiana*. 43: 1573–1582.
- Bennani, F. and Husson, E. 2001. Impedance spectroscopy analysis of pure and Ni-doped lithium tantalate. *Journal of the European Ceramic Society*. 21:847–854.
- Bharadwaj, S.R., Varma, S. and Wani, B.N. 2012. Electroceramics for fuel cells, batteries and sensors, India.
- Biswas, S. P., Tangri, R. P., Prasad, R., and Suri, a. K. 2000. Microwave Assisted Synthesis of LiNbO₃ and LiTaO₃. *Transactions of the Indian Ceramic Society*. 59: 88–91.
- Blasse, G. 1964a. On the Structure of some Compounds Li₃M(V)O₄, and some other Mixed Metal Oxides Containing Lithium. *Zeitschrift für anorganische und allgemeine Chemie*, 331:44–50.
- Blasse, G. 1964b. On the Structure of some Compounds Li₃Me(5+)O₄, and some other Mixed Metal Oxides Containing Lithium. *Zeitschrift für anorganische und allgemeine Chemie*. 331:44–50.
- Bohnke, O. 2008. The fast lithium-ion conducting oxides Li_{3x}La_{2/3-x}TiO₃ from fundamentals to application. *Journal of Solid State Ionics*. 179: 9–15.
- Borisevich, A. and Davies, P.K. 2001. Microwave dielectric properties of Li_{1+x-y}M_{1-x-3y}Ti_{x+4y}O₃ (M = Nb⁵⁺, Ta⁵⁺) solid solutions. *Journal of European ceramic society*. 21: 1719–1722.
- Borisevich, A. Y. and Davies, P. K. 2002. Crystalline Structure and Dielectric Properties of Li_{1+x-y}Nb_{1-x-3y}Ti_{x+4y}O₃ M-Phase Solid Solutions. *Journal of America Ceramic Society*. 85: 573–578.

- Boulay, Sakaguchi, D. du, Ishizawa, A., Suda, K. and Nobuo. 2003. Reinvestigation of β -Li₃TaO₄. *Journal of Acta Crystallographica Section E Structure Reports Online*. 59: i80–i82
- Brabers, V.A.M. 1969. Infrared Spectra of Cubic and Tetragonal Manganese Ferrites. *Journal of hysica Status Solidi (B)*. 33:563–572.
- Bruce, P.G. and West, A.R. 1982. Ionic conductivity of LISICON solid solutions, Li_{2+2x}Zn_{1-x}GeO₄. *Journal of Solid State Chemistry*. 44: 354–365.
- Bruce, P. G. 1983. The A-C Conductivity of Polycrystalline LISICON, Li_{2+2x}Zn_{1-x}GeO₄ and a Model for Intergranular Constriction Resistances. *Journal of The Electrochemical Society*. 130: 662.
- Chen, C. F., Llobet, A., Brennecke, G. L., Forsyth, R. T., Guidry, D. R., Papin, P. A., and McCabe, R. J. 2012. Powder synthesis and hot-pressing of a LiTaO₃ ceramic. *Journal of the American Ceramic Society*. 1–7.
- Chen, X M. 1996. “Crystallization Characteristics of LiNbO₃ Derived from Sol Gel.” *Journal of Materials Sciences science* 7: 51–54.
- Chon, M. P., Tan, K. B., Khaw, C. C., Zainal, Z., Yap, Y. H. T., Chen, S. K. and Tan, P. Y. 2014. Investigation of the phase formation and dielectric properties. *Journal of Alloys and Compounds*, 590: 479–485.
- Cole, K.S. and Cole, R.H. 1941. Dispersion and Absorption in Dielectrics - I Alternating Current Characteristics. *Journal of Chemistry. Physics*. 9: 341–352.
- Cox, D.E., Takei, W.J. and Shirane, G. 1962. *American Crystallography Association: Programme and Abstracts*, L6
- Dash, U., Sahoo, S., Parashar, S.K.S. and Chaudhuri, P. 2014). Effect of Li⁺ ion mobility on the grain boundary conductivity of Li₂TiO₃ nanoceramics. *Journal of Advanced Ceramics*. 3: 98–108.
- Delmas, C., Maazaz, A., Guillen, F., Fouassier, C. and Reau, J. M. 1979. Des conducteurs ioniques pseudo-dimensionnels: Li₈MO₆ (M=Zr, Sn), Li₇LO₆ (L = Nb, Ta) et Li₆In₂O₆. *Journal of Materials Research Bulletin*. 14: 619–625.
- Deqiong, Z., Shuming, P., Xiaojun, C., Xialing, G. and Tongzai, Y. 2010. Fabrication and characterization of Li₃TaO₄ ceramic pebbles by wet process. *Journal of Nuclear Materials*. 396: 245–250.
- El-Bachiri, A., Bennani, F. and Boussemamti, M. 2014. Dielectric and electrical properties of LiNbO₃ ceramics. *Journal of Asian Ceramic Societies*, 4: 46–54.
- Elouadi, B. and Zriouil, M., 1981. Some new non-stoichiometric ferroelectric phases appearing close to LiTaO₃ in the ternary systems Li₂O-Ta₂O₅-(TiO₂)₂. *Materials Research Bulletin*, 16: 1099–1106.

- Eloudi, B. and Zriouil, M., 1986. Investigation of the crystal chemical and ferroelectric properties the vicinity of LiNbO_3 and LiTaO_3 inside the ternary Systems $\text{Li}_2\text{O-Nb}_2\text{O}_5\text{-(TiO}_2)_2$ and $\text{Li}_2\text{O-Ta}_2\text{O}_5\text{-(SnO}_2)_2$. *Journal of Solid State Chemistry*, 64: 22–29
- Fallon, G. D., Gatehouse, B. M., Roth, R. S. and Bureau, N. 1979. Crystal Structures of Some Niobium and Tantalum Oxides, Part VI. The Structure of $\text{H-LiTa}_3\text{O}_8$. *Journal of Solid State Chemistry*. 27: 255–259.
- Fehr, T. and Schmidbauer, E. 2007. Electrical conductivity of Li_2TiO_3 ceramics. *Solid State Ionics*, 178 :35–41.
- Grabmaier, B. C. and F. Otto, 1986. Growth and Investigation of MgO-Doped LiNbO_3 . *Journal of Crystal Growth* 79:682–688.
- Gabriella, D. 2008. Study of the phase equilibria in the ternary systems $\text{X}_2\text{O-Li}_2\text{O-Nb}_2\text{O}_5$ (X = Na , Rb , Cs), single crystal growth and characterization of LiNbO_3 , PhD thess
- Garcia-Martin, S., Rojo, J. M., Tsukamoto, H., Moran, E., and Alario-Franco, M.A. 1999. Lithium-ion conductivity in the novel $\text{La}_{1/3-x}\text{Li}_{3x}\text{NbO}_3$ solid solution with perovskite-related structure. *Journal of Solid State Ionics*. 116: 11–18.
- Gatehouse, B.M., Negas, T. and Roth, R.S. 1976. The crystal structure of $\text{M-LiTa}_3\text{O}_8$ and its relationship to the mineral wodginite. *Journal of Solid State Chemistry*, 18: 1–7.
- Ginnings, D.C. and Phipps, T. E. 1930. Temperature-conductance curves of solid salts. III. halides of lithium. 52:1340–1345.
- Glass, A. M., Nassau, K. and Negran, T. J. 1978. Ionic conductivity of quenched alkali niobate and tantalate glasses. *Journal apply physics*. 49: 4808–4811.
- Hakki, B.W., and P.D. Coleman. 1960. “A Dielectric Resonator Method of Measuring Inductive Capacities in the Millimeter Range.” *IEEE Transactions on Microwave Theory and Techniques*. 8: 402–10.
- Heed, B., Lunden, A. and Schroeder, K. 1975. Sulfate-based solid electrolyte as a new alternative for power sources. Intersoc. Energy Convers Eng. Conf, 10th, Rec, Newark, DE. USA.
- Hodge, I.M., Ingram, M.D. and West, A.R. 1976. Impedance and modulus spectroscopy of polycrystalline solid electrolytes. *Journal of Electroanalytical Chemistry*, 74:125–143.
- Hodge, M., Ingram, M.D. and West, A.R. 1976. Ionic Conductivity of Li_4SiO_4 , Li_4GeO_4 and and Their Solid Solutions. *Journal of American Ceramic Society*. 59: 7-8
- kuwana, H.Y.P. 1978. Crystal structure and ionic conductivity of $\text{Li}_{14}\text{Zn}(\text{GeO}_4)_4$ and other new Li^+ superionic conductors. *Materials Research Bulletin*. 13: 117-124.

- Hsiao, Y. J., Fang, T. H., Lin, S. J., Shieh, J. M., and Ji, L. W. 2010. Preparation and luminescent characteristic of Li_3NbO_4 nanophosphor. *Journal of Luminescence*, 130: 1863–1865
- Huanosta, A. and West, A.R. 1987. The electrical properties of ferroelectric LiTaO_3 and its solid solutions. *Journal of Applied Physics*. 61: 5386–5391.
- Huggins, R.A. (1977). Recent results on lithium ion conductors. *Electrochimica Acta*. 22:773-881.
- Inaguma, Y., Liqun, C., Itoh, M., Nakamura, T., Uchida, T., Ikuta, H. and Wakihara, M. 1993. High ionic conductivity in lithium lanthanum titanate. *Solid State Communications*. 8: 689-693.
- Irvine, J. T. S., Sinclair, D. C., and West, A. R. 1990. Electroceramics: characterization by impedance spectroscopy. *Journal of Advanced Materials*. 2: 132–138.
- Iyi, N., Kitamura, K., Yajima, Y., Kimura, S., Furukawa, Y. and Sato, M. 1995 Defect structure model of MgO-Doped LiNbO_3 . *Journal of Solid State Chemistry*. 118:148–152.
- Jahnberg, L. and Andersson, S. 1967. Studies on Pentavalent Tantalum Oxide fluoride and the Thermal Decomposition of TaO_2F . *Journal of Acta Chemica Scandinavica*, 21: 615–619.
- Janot, R. and Guérard, D. 2005. Ball-milling in liquid media: Applications to the preparation of anodic materials for lithium-ion batteries. *Progress in Materials Science*. 50 : 1–92.
- Jie, Z., Dongxu, L., Wei, D., Zeyan, W., Peng, W., Hefeng, C. and Minhua, J. 2011. Synthesis and characterization of high crystallinity, well-defined morphology stoichiometric lithium niobate nanocrystalline. *Journal of Crystal Growth*. 318: 1121–1124.
- Kalhammer, F.R., Kozawa, A., Moyer, C.B. and Owens, B.B. 1996. Electrochemistry Society, Interface.
- Kashif, I., Soliman, A. a., Sakr, E. M. and Ratep, A. 2013. XRD and FTIR studies the effect of heat treatment and doping the transition metal oxide on LiNbO_3 and LiNb_3O_8 nano-crystallite phases in lithium borate glass system. *Spectrochimica Acta - Part A: Molecular and Biomolecular Spectroscopy*. 113: 15–21.
- Kobayashi, Y., and M. Katoh. 1985. “Microwave Measurement of Dielectric Properties of Low-Loss Materials by the Dielectric Rod Resonator Method.” *IEEE Transactions on Microwave Theory and Techniques* 33: 586–92.
- Koller, A. (1994). Structure and properties of Ceramics. (A. Koller, Edition). Czech Republic: Elsevier Science Publishers.
- Krichen, M., Megdiche, M., Guidara, K., and Gargouri, M. 2015. AC conductivity and mechanism of conduction study of lithium barium pyrophosphate $\text{Li}_2\text{BaP}_2\text{O}_7$ using impedance spectroscopy. *Journal of Ionics*. 21: 935–948.

- Kumar, P.P. and Yashonath, S. 2006. Ionic Conduction in the Solid State. *Journal of Chemical Sciences*, 118:135–54.
- Lanfredi, S. and Rodrigues, a. C.M. 1999. Impedance spectroscopy study of the electrical conductivity and dielectric constant. *Journal of Applied Physics*, 86: 2215.
- Lee, C. K. and West. A.R. 1991. Liquid-like Lithium Ion Conductivity in $\text{Li}_{4-3x}\text{Al}_x\text{GeO}_4$ solid electrolyte, *Journal Material Chemistry*, 1:149–50.
- Lee, C.K. and Hong, B. (2010). New oxide ion conducting solid electrolytes , $\text{Bi}_4\text{V}_2\text{O}_{11}$: , 6: 331–335.
- Lee, S. L., Lee, C. K., Sinclair, D. C., Chong, F. K., Halim, S. A., and Yap, T. 2005. Preparation and Characterization of New Oxide Ion Conductors in Bi_2O_3 - As_2O_5 System. *Malaysian Journal of Chemistry*, 7, 001–010.
- Lemine, O. M. 2009. Microstructural characterisation of α - Fe_2O_3 nanoparticles using, XRD line profiles analysis, FE-SEM and FT-IR. *Superlattices and Microstructures*, 45, 576–582.
- Liu, Zhifu, Wang, Y., Wenjun, W. and Yong, X.L. 2013. “Li–Nb–Ti–O Microwave Dielectric Ceramics.” *Journal of Asian Ceramic Societies* 1: 2–8.
- Luiz, A.D., Filho, M., Yang, H., Downs, R. T., C., C. L. S., and Persiano, A. C. 2012. Lithiotantite, ideally LiTa_3O_8 . *Journal of Acta Crystallographica Section E Structure Reports Online*, 68: i27–i28.
- Lundberg, M. 1965. The Crystal Structure of $\text{LiNb}_6\text{O}_{11}\text{F}$. *Journal of Acta Chemica Scandinavica*. 19: 2274–2284.
- Lundberg, M. and Andersson, S. 1965. Phase analysis Stuides in the $\text{LiF-Nb}_2\text{O}_5$ system. *Journal of Acta Chemica Scandinavica*. 19:1376–1380.
- Lundberg, M. 1972. The crystal structure of Nb_2WO_8 . *Journal of Acta Chemica Scandinavica*. 26: 2932–2940.
- Lunden, A. Chowdari and Radhakrishna, S. 1986. Batteries, Sensors and Heat Storage Materials for Solid State Batteries. World Science Pub. Co. Singapore.
- Macdonald, J.R. and Barsoukov, E. 2005. Impedance spectroscopy theory, experiment, and applications, second ed., pp 9. A John Wiley & Sons, Inc., Publication.
- Manthiram, A. 2011. Materials challenges and opportunities of lithium ion batteries. *Journal of Physical Chemistry Letters*, 2:176–184.
- Martel, L.C and Roth, R.S. 1981. American Chemical Society Bulletin. 60: 37
- Mather, G. C., Dussarrat, C., Etourneau, J. and West, A. R. 2000. A review of cation-ordered rock salt superstructure oxides. *Journal of Royal Science of Chemistry*. 10: 2219–2230.

- McLaren, V. L., Kirk, C. a, Poisot, M., Castellanos, M., and West, A. R. 2004. Li(+) ion conductivity in rock salt-structured nickel-doped Li_3NbO_4 . *Dalton Transactions (Cambridge, England. (19):* 3042–3047.
- Megaw, H.D. 1968. “A Note on the Structure of Lithium Niobate, LiNbO_3 .” *Acta Crystallographica A*24: 583–88.
- Miao, C. R. and Torardi, C. C. 1999. X-ray and ultraviolet luminescence of $\text{Li}_3\text{Ta}_{1-x}\text{Nb}_x\text{O}_4$ prepared by flux synthesis and characterization of a new high efficiency X-ray phosphor. *Journal of Solid State Chemistry. 145:* 110–115.
- Mohammadi, M.R. and Fray, D.J. 2009. Low-temperature perovskite-type cadmium titanate thin films derived from a simple particulate sol-gel process. *Journal of Acta Materialia, 57:*1049–1059.
- Moulson, A . J. and Herbert, J. M. 2003. *Electroceramics: Materials, Properties Applications*.second edition, John Wiley & sons.
- Muhle, C., Dinnebier, R. E., Wullen, L. Van, Schwering, G. and Jansen, M. 2004. New insights into the structural and dynamical features of lithium hexaoxometalates Li_7MO_6 (M= Nb,Ta,Sb,Bi). *Journal of Inorganic Chemistry. 43:* 619–625.
- Murugan, R., Thangadurai, V. and Weppner, W. 2008. Lattice Parameter and Sintering Temperature Dependence of Bulk and Grain-Boundary Conduction of Garnet-like Solid Li-Electrolytes. *Journal of The Electrochemical Society. 155:*A90–A101.
- Nomura, E. and Greenblatt, M. 1984. Ionic conductivity of substituted Li_7TaO_6 phases. *Journal of Solid State Ionics. 13:* 249–254.
- Nord, A.G. and Thomas, J.O.1978. Structural studies of the solid electrolyte high- LiTa_3O_8 . *Journal of Acta chemica Scandinavica, A32:* 539–544.
- Ono, H., Hosokawa, Y., Shinoda, K., Koyanagi, K. and Yamaguchi, H. 2001. Ta-O phonon peaks in tantalum oxide films on Si. *Journal of hin Solid Films, 57–61.*
- Owens, B.B. and Salkind, A.J. 1986. Batteries for implantable Biomedical Devices, Plenum, New York, Chapter 2.
- Pang, L.-X., Liu, H., Zhou, D., Yang, J.-X., Li, D.-J., and Liu, W.G. 2012. Low-temperature sintering and microwave dielectric properties of Li_3MO_4 (M = Ta, Sb) ceramics. *Journal of Alloys and Compounds. 525:* 22–24.
- Polgár, K., Kovács, L., Földvári, I., and Cravero, I. 1986. Spectroscopic and electrical conductivity investigation of Mg doped LiNbO_3 single crystals. *Solid State Communications, 59:*375–379.
- Prakash, B.J. and Buddhudu, S. 2012. Synthesis and analysis of LiNbO_3 ceramic powders by co-precipitation method. *Indian Journal of Pure & Applied Physics. 50:*320–324.

- Qu, Q. T., Wang, B., Yang, L. C., Shi, Y., Tian, S., and Wu, Y. P. 2008. Study on electrochemical performance of activated carbon in aqueous Li_2SO_4 , Na_2SO_4 and K_2SO_4 electrolytes. *Electrochemistry Communications*, 10:1652–1655.
- Rahmouni, H., Nouiri, M., Jemai, R., Kallel, N., Rzigua, F., Selmi, A. and Alaya, S. 2007. Electrical conductivity and complex impedance analysis of 20% Ti-doped $\text{La}_{0.7}\text{Sr}_{0.3}\text{MnO}_3$ perovskite. *Journal of Magnetism and Magnetic Materials*. 316:23–28.
- Reisman, A. and Holtzberg, F. 1958. Heterogeneous equilibria in the systems $\text{Li}_2\text{O}-\text{Ag}_2\text{O}-\text{Nb}_2\text{O}_5$ and oxide-models. *Journal of American Chemical Society*. 80: 6503–6507.
- Reisman, A. 1961. Compound repetition in oxide systems, solid phases in the system $\text{Li}_2\text{O}-\text{Ta}_2\text{O}_5$ and $\text{Na}_2\text{O}-\text{Ta}_2\text{O}_5$. *Journal physics chemistry*. 66:15.
- Rice, C. E., and Holmes, R. J. 1986. A new rutile structure solid-solution phase in the $\text{LiNb}_3\text{O}_8-\text{TiO}_2$ system, and its role in Ti diffusion into LiNbO_3 . *Journal of Applied Physics*. 60: 3836–3839.
- Rickert, H. 1978. Solid Ionic Conductors: Principles and Applications. *Angewandte Chemie International Edition in English*, 17:37–46.
- Roth, R.S., Parker, H.S., Brower, W.S., and Waring, J.L. 1972. Fast Ion Transport in Solid. *Study Institute, Belgirate, Italy, North-Holland, Amsterdam*, 1973
- Samuel, V., Gaikwad, A. B., Jadhav, A. D., Mirji, S. A. and Ravi, V. 2007. A novel technique to prepare LiNbO_3 at low temperature. *Journal of Materials Letters*, 61: 765–766.
- Setter, N. and Waser, R. 2000. Electroceramic materials. *Journal of Acta Material*, 48: 151–178.
- Setter, Nava. 2001. Electroceramics : Looking Ahead. *Journal of The Electrochemical Society*, 21:1279–93.
- Shishido, T., Suzuki, H., Ukei, K., Hibiya, T. and Fukuda, T. 1996. Flux growth and crystal structure determination of trilithium niobate. *Journal of Alloys and Compounds*, 234: 256–259.
- Sinclair, D. C. and West, A. R. 1989. Impedance and modulus spectroscopy of semiconducting BaTiO_3 showing positive temperature coefficient of resistance. *Journal of Applied Physics*. 66: 3850–3856.
- Sinclair, D. C. 1995. Characterization of Electro-materials using ac Impedance Spectroscopy. *Journal of Applied Physics*. 65: 55–66.
- Singh, R., Bahel, S. and Bindra-Narang, S. 2017. Dielectric and optical study of the M-phase LNT ($\text{Li}-\text{Nb}-\text{Ti}-\text{O}$) solid solutions. *Journal of Materials Research Bulletin*. 88: 200–205.

- Smith, R.I. and West, A.R., 1992. Characterisation of an incommensurate LiTiNb oxide. *material response Bulletin*, 27: 277–285.
- Song, Y. J., Zhang, Q. H., Shen, X., Ni, X. D., Yao, Y., and Yu, R. C. 2014. Room-temperature magnetism realized by doping Fe into ferroelectric LiTaO₃. *Chinese Physics Letters*, 31.
- Staffanson, L. 1972. The Phase Diagram Li₂SO₄-Na₂SO₄. *Acta Chemica Scandinavica*. 26: 2150.
- Subasri, R. and Sreedharan, O.M. 1997. High-temperature thermodynamic stability of LiTa₃O₈ from emf measurements using alpha-beta alumina as solid electrolyte. *Journal of Materials Letters*. 30: 289–292.
- Svaasand, L. O., Eriksrud, M., Grande, A. P., and MO, F. 1973. Crystal growth and properties of LiNb₃O₈. *Journal of Crystal Growth*. 18: 179–184.
- Tarneberg, R. and Lundêr, A. (1996). Ion diffusion in the high-temperature phases Li₂SO₄, LiNaSO₄, LiAgSO₄ and Li₄Zn(SO₄)₃. *Solid State Ionic*. 90: 209-220.
- Thangadurai, V. and Weppner, W. 2002. Solid state lithium ion conductors: Design considerations by thermodynamic approach. *Journal of Ionics*. 8: 281–292.
- Torii, Y., Sekiya, T., Yamamoto, T., Koyabashi, K., and Abe, Y. 1983. Preparation and properties of LiTaO₃-based solid solutions with cation vacancies. *Journal of Materials Research Bulletin*. 18. 1569–1574.
- Ukei, K., Suzuki, H., Shishido, T. and T. Fukuda, T. 1994. Li₃NbO₄. *Journal of Acta crystallographica*. C50: 655–656.
- Vilarinho, P. M., Barroca, N., Zlotnik, S., Félix, P., and Fernandes, M. H. 2014. Are lithium niobate (LiNbO₃) and lithium tantalate (LiTaO₃) ferroelectrics bioactive? *Materials science & engineering. C, Journal Of Materials for biological applications*. 39: 395–402.
- Villafuerte-castrejon, M.E., Arogon-Pina, A., Valenzuela, R. and West, A.R., 1987. Compound and solid Solution formation in the syatem Li₂O-Nb₂O₅-Ti₂O. *Journal of Solid State Chemistry*, 71: 103–108.
- Wachs, I. E., Briand, L. E., Jehng, J.-M., Burcham, L. and Gao, X. 2000. Molecular structure and reactivity of the group V metal oxides. *Journal of Catalysis Today*. 57: 323–330.
- West, A.R. 1973. Ionic conductivity of oxides based on Li₄SiO₄. *Journal of Applied Electrochemistry*. 3: 327-335.
- West, A.R. 1984. Ionic conductivity and solid electrolytes. In solid state chemistry and its applications. Edition A.R.West. New York: John Wiley & Sons, Ltd
- West, A.R. 1999. Basic solid state chemistry, second edition, Chichester: John Wiley and Sons.

- West, Anthony R., Timothy B. Adams, Finlay D. Morrison, and Derek C. Sinclair. 2004. Novel High Capacitance Materials BaTiO₃La and CaCu₃Ti₄O₁₂. *Journal of the European Ceramic Society*. 24:1439–48.
- Whiston, C.D. and Smith, A.J. 1965. Double Oxides Containing Niobium or Tantalum. I. Systems Including Alkali Metals. *Acta Crystallographica*, 19: 169–173.
- Williamson, G. ., and Hall, W. . 1953. X-ray Line Broadening from Filled Aluminium and Wolfram. *Acta Metallurgica*, 1: 22–31.
- Yang, T., Liu, Y. G., Zhang, L., Hu, M. L., Yang, Q., Huang, Z. H., and Fang, M. H. 2014. Powder synthesis and properties of LiTaO₃ ceramics. *Journal of Advanced Powder Technology*.25: 933–936.
- Ye, Z. G., Von Der Mühl, R., Ravez, J., and Hagenmuller, P. 1988. Dielectric, piezoelectric, and pyroelectric studies of LiTaO₃-derived ceramics sintered at 900 °C following the addition of (LiF + MgF₂). *Journal of Materials Research*. 3: 112–115.
- Yogamalar, R., Mahendran, V., Srinivasan, R., Beitollahi, A., Kumar, R. P., Bose, A. C. and Vinu, A. 2010. Gas-sensing properties of needle-shaped Ni-doped SnO₂ nanocrystals prepared by a simple sol-gel chemical precipitation method. *Chemistry - An Asian Journal*. 5: 2379–2385.
- Yoon, S. O., Yoon, J. H., Kim, K. S., Shim, S. H., and Pyeon, Y. K. 2006. Microwave dielectric properties of LiNb₃O₈ ceramics with TiO₂ additions. *Journal of the European Ceramic Society*. 26: 2031–2034.
- Yu, J. C., Zhang, L., Zheng, Z., and Zhao, J. 2003. Synthesis and Characterization of Phosphated Mesoporous Titanium Dioxide with High Photocatalytic Activity Synthesis and Characterization of Phosphated Mesoporous Titanium Dioxide with High Photocatalytic..(15):2280–2286.
- Zainuddin, L.W. and Kamarulzaman, N. 2012. Impedance spectroscopy study of litao₃ powder synthesized via solgel method. *Journal of Advanced Materials Research*. 545: 275–278.
- Zhang, J.-Y., Fang, Q. and Boyd, I. W. 1999. Growth of tantalum pentoxide film by pulsed laser deposition. *Journal of Applied Surface Science*, 138–139: 320–324.
- Zhang, D. R., Liu, H. L., Jin, R. H., Zhang, N. Z., Liu, Y. X., and Kang, Y. S. 2007. Synthesis and Characterization of Nanocrystalline LiTiO₂ Using a One-Step Hydrothermal Method, 13, 92–96.
- Zhou, D., Wang, H., Pang, L. X., Yao, X. and Wu, X. G. 2008. Microwave Dielectric Characterization of a Li₃NbO₄ Ceramic and Its Chemical Compatibility with Silver. *Journal of American Ceramic Society*. 91: 4115–4117.
- Zhou, H., Chen, X., Fang, L., and Chu, D. 2010. Low temperature cofiring and compatibility with silver electrode of Li 3NbO₄ ceramics with B₂O₃ addition. *Japanese Journal of Applied Physics*. 49:3–7.

Zhou, W. 1992. Structural chemistry and physical properties of some ternary oxides in the Bi_2O_3 - Ta_2O_5 system. *Journal of Solid Chemistry*. 101: 1-17.

Ziman J.M., *Physical Sciences.*, Calrendo Press, Oxford, (2001), 1960.

Zocchi, M. and Gatti, M. 1983. Neutron and X-ray diffraction study on polymorphism in lithium orthotantalate, Li_3TaO_4 . *ournal of Solid State Chemistry*. 48: 420–430.

